Desalination and Water Treatment
www.deswater.com
51 (2013) 1468–1476
February
1944-3994/1944-3986
doi: 10.1080/19443994.2012.699350
Taylor & Francis
Taylor & Francis Group

Geochemical modeling of groundwater in the El Eulma area, Algeria

Lazhar Belkhiri[a,*], Lotfi Mouni[b]

[a]*University Hadj Lakhdar, 05000 Batna, Algeria*
Tel. +213 95947853; email: belkhiri_laz@yahoo.fr
[b]*Département des Sciences Techniques, Institut des Sciences, Université Akli Mohand Oulhadj, Bouira, Algeria*

Received 24 February 2012; Accepted 29 May 2012

ABSTRACT

Multivariate statistical and geochemical modeling techniques were used to determine the main factors and mechanisms controlling the chemistry of groundwaters in the El Eulma area. Three major water groups resulted from the Q-mode cluster analysis. The samples from the area were classified as low salinity (Group 1), moderate salinity (Group 2), and high salinity waters (Group 3). Inverse geochemical models of the statistical groups were developed using PHREEQC to elucidate the chemical reactions controlling water chemistry. In a broad sense, the reactions responsible for the hydrochemical evolution in the area fall into three categories: (1) dissolution of evaporite minerals; (2) precipitation of carbonate minerals, quartz, kaolinite, and Ca-smectite; and (3) ion exchange.

Keywords: Q-mode cluster analysis; Water–rock interaction; Geochemical modeling; El Eulma area; Algeria

1. Introduction

Groundwater is one of the most important resources for human life. The water quality depends upon the geological environment, natural movement, recovery, and utilization. The chemical quality of the groundwater percolating through the soil zones of anthropogenically polluted layers are significantly reduced. Hence, understanding the groundwater quality changes, solute transport, and identifying recharge areas in the groundwater zone have become important in protecting human health. This is because groundwater contains a wide variety of dissolved inorganic species in various concentrations, as a result of chemical and biochemical interactions between groundwater and geological materials through which it flows; and to a lesser extent because of contributions from the atmosphere, surface water bodies, and anthropogenic activities.

Multivariate techniques have been used to resolve hydrological factors such as aquifer boundaries, groundwater flow paths, and hydrochemical parameters (e.g. [1–7]), to identify geochemical controls on the composition [8,9] and to separate anomalies such as anthropogenic impacts from background [10–13]. Hierarchical cluster analysis as a multivariate statistical tool has also been widely used to formulate geochemical models on the basis of available data.

Inverse geochemical modeling in PHREEQC [14] is based on a geochemical mole-balance model, which calculates the phase mole transfers (the moles of

*Corresponding author.

Presented at the International Conference on Desalination for the Environment, Clean Water and Energy, European Desalination Society, 23–26 April 2012, Barcelona, Spain

minerals and gases that enter or leave a solution) to account for the differences in an initial and a final water composition along the flow path in a groundwater system. At least two chemical analyses of groundwater at different points of the flow path and a set of phases (minerals and/or gases) which potentially react along this flow path are needed to populate the program [15]. A number of assumptions are inherent in the application of inverse geochemical modeling: (1) the two groundwater analyses from the initial and final water wells should represent groundwater that flows along the same flow path, (2) dispersion and diffusion do not significantly affect groundwater chemistry, (3) a chemical steady state prevails in the groundwater system during the time considered, and (4) the mineral phases used in the inverse calculation are or were present in the aquifer [16]. The soundness or validity of the results in the inverse modeling depends on a valid conceptualization of the groundwater system, validity of the basic hydrochemical concepts and principles, accuracy of input data into the model, and level of understanding of the geochemical processes in the area [17]. This study intends to examine the variations of groundwater chemistry of the study area as well as interpret the processes that control the groundwater chemistry.

2. Study area

The area of study is located in the East of Algeria (Fig. 1). The climate of the study area is considered to be semi arid, the annual precipitation being approximately 421 mm. The rainy season extends from October to May, with a maximum during December and March off each year. The mean monthly temperatures vary between −3 and 38°C, the mean annual value being 15°C. The vegetation of the study area is characterized by grasses and herbs. Soils are generally sandy to clayey in texture and mostly classified as Aridisol and are calcareous. Mineralogically, most of the soils are dominated by kaolinite, illite, smectite, and chlorite—typical for most arid and semi-arid soils. The presence of smectite suggests specific sites for sodium adsorption. Most of its inhabitants are concentrated in the town of El Eulma with more than 30,000 working mainly in the production of cereals (barley and corn).

Rocks and unconsolidated deposits in the area can be divided into three geologic units [18–21]: (1) upper Cretaceous (Senonian); (2) Eocene; and (3) Mio-Plio-Quaternary. Senonian (upper Cretaceous) is generally found in the northern part of the study area. Senonian units are composed of Santonian-Campanian formation and upper Senonian formation. These formations consist of various rocks with differing compositions

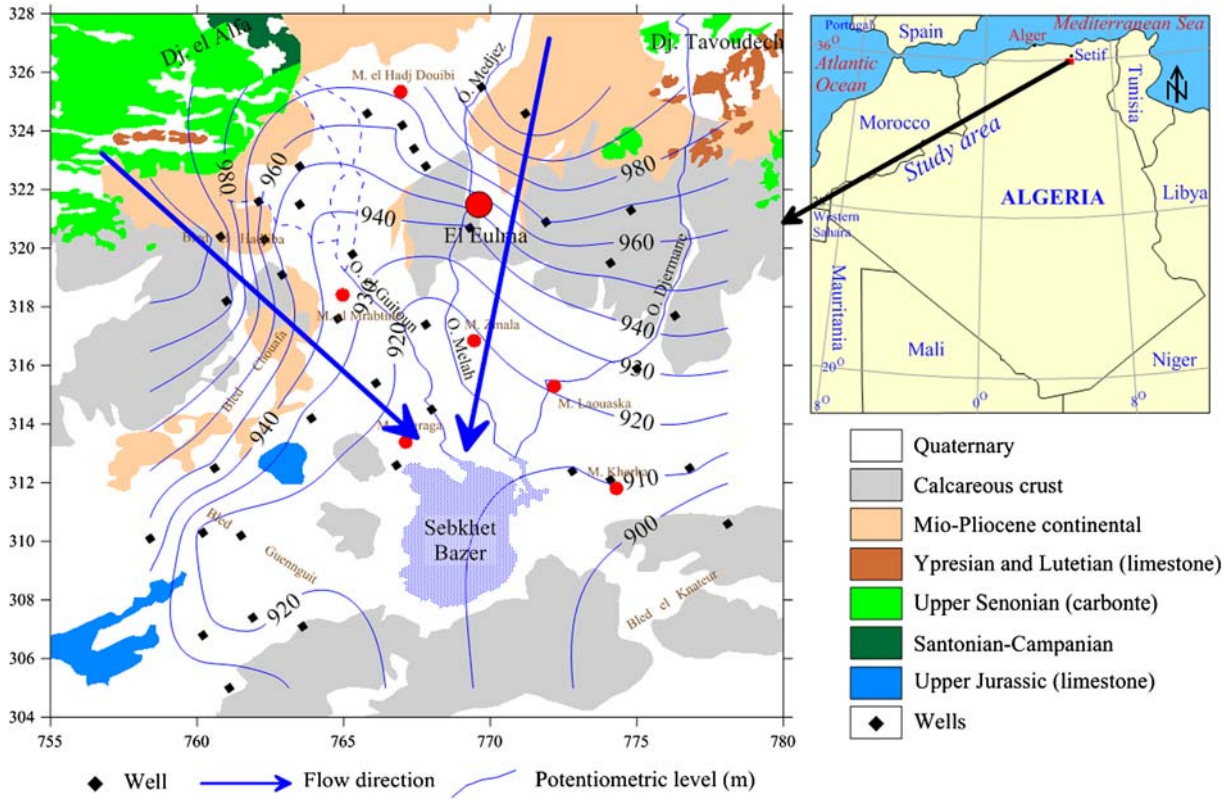

Fig. 1. Map showing water sampling locations and geology of the studied area.

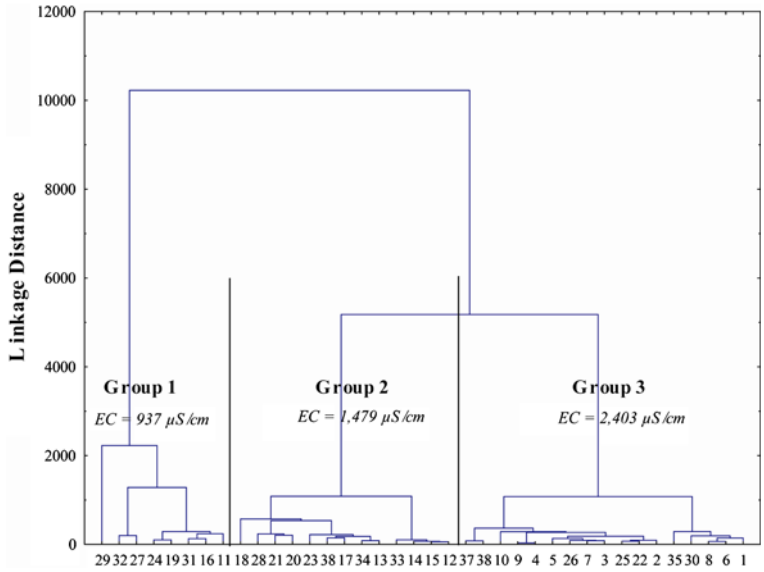

Fig. 2. Dendogram of Q-mode CA.

including limestone and marl of about 550 m thick. Eocene units are composed of Ypresian–Lutetian formation (Fig. 1). Eocene rocks consist of a succession of marine, limestone, and silt of about 80 m thick. The Mio-Plio-Quaternary is a heterogeneous continental detrital sedimentation.

The studied area is situated in the alluvial plain of the Mio-Plio-Quaternary. Shallow groundwater mainly forms 5–80 m below the surface. Groundwater is recharged by vertical infiltration meteoric water in the basin and by stream water coming from different reliefs surrounding the depression intermountainous of El Eulma. Evapotranspiration and artificial abstraction are the major processes of shallow groundwater discharge. The direction of groundwater flow around El Eulma plain is from south to NE-SW in east and from north to NW-SE in west. In general, the groundwater flows toward the center of the plain (Fig. 2). The pumping tests on different wells showed high transmissivity (10^{-3} m^2/s) indicating high yields.

3. Materials and methods

3.1. Water samples

For this study, a set of 38 groundwater samples was analyzed for 11 physical and chemical parameters comprising major ion concentrations (Ca^{2+}, Mg^{2+}, Na^+, K^+, Cl^-, SO_4^{2-}, HCO_3^-, NO_3^-), electrical conductivity (EC), pH, and the temperature (T). The samples were taken from wells located in the El Eulma aquifer, East Algeria (Fig. 1). The samples were collected after pumping for 10 min. This was done to remove groundwater stored in the well. These samples were collected using 4–1 acid-washed polypropylene containers. Each sample was immediately filtered on site through 0.45 µm filters on acetate cellulose. Filtrate for metals analyses was transferred into 100-cm^3 polyethylene bottles and immediately acidified to pH < 2 by the addition of Merck™ ultrapure nitric acid (5 ml 6 N HNO_3). Samples for anions analyses were collected into 250-cm^3 polyethylene bottles without preservation. All the samples were stored in an ice chest at a temperature <4 °C and later transferred to the laboratory and stored in a refrigerator at a temperature <4 °C until analyzed (within 1 week). Immediately after sampling, temperature, pH, and EC were measured in the field using a multi-parameter WTW (P3 MultiLine pH/LF-SET). Subsequently, the samples were analyzed in the laboratory for their chemical constituents such as calcium, magnesium, sodium, potassium, chloride, bicarbonate, sulfate, and nitrate. This was achieved using standard methods as suggested by the American Public Health Association [22–24]. Ca^{2+}, Mg^{2+}, HCO_3^-, and Cl^- were analyzed by volumetric titrations. Concentrations of Ca^{2+} and Mg^{2+} were estimated titrimetrically using 0.05 N EDTA and 0.01 N, and those of HCO_3^- and Cl^- were estimated by H_2SO_4 and $AgNO_3$ titration, respectively. Concentrations of Na^+ and K^+ were measured using a flame photometer (Model: Systronics Flame Photometer 128) and that of sulfate (SO_4^{2-}) by turbidimetric method [25]. Nitrate (NO_3^-) was analyzed by colorimetry with a UV–visible spectrophotometer [26]. Standard solutions for the above analysis were prepared from the respective salts of analytical reagents grade. The accuracy of the

chemical analysis was verified by calculating ion balance errors, where the errors were generally within 10%.

3.2. Data treatment and multivariate statistical method

Groundwater quality data-sets were subjected to the multivariate technique (cluster analysis [CA]). CA is the name given to an assortment of techniques designed to perform classification by assigning observations to groups, so each is more-or-less homogeneous and distinct from other groups [27]. As an exploratory technique with graphic output, CA does not require the assumptions that other statistical methods do, except that the data were heterogeneous. It provided a self-explanatory graphic display (dendrogram), and was a method used frequently in the geological sciences to help classify or group samples/variables of a data-set. It helped to identify natural groupings for samples (Q-mode), and in turn, reduced the size of the samples/variables into smaller numbers of groups. Hydrochemical results of all samples were statistically analyzed by using the software [28].

4. Results and discussion

4.1. General water chemistry

The pH value of groundwater in the study area ranges from 7.8 to 8.5, indicating an alkaline type of groundwater (Table 1). The EC of groundwater samples ranges from 608 to 3,577 μS/cm with a mean value of 1,431 μS/cm. The mean temperature of water was 11.16 °C. The relative abundance of the ions is $Ca^{2+} > Na^{2+} > Mg^{2+} > K^{+}$ (on molar basis) and $Cl^{-} > HCO_3^{-} > SO_4^{2-} > NO_3^{-}$ (Table 1). The maximum concentration of Ca^{2+} and Mg^{2+}—288.6 and 74.13 mg/l, respectively—are, however, higher than their respective [29] standards of 75 and 30 mg/l. The mean sodium and potassium concentrations in the groundwater are 105.69 and 4.54 mg/l, respectively. Bicarbonate ion represents the second dominance anion in the

Table 1
Chemical summary of shallow groundwater in the study area

	EC	*T*	pH	Ca^{2+}	Mg^{2+}	Na^{+}	K^{+}	Cl^{-}	SO_4^{2-}	HCO_3^{-}	NO_3^{-}
Min	608	7.9	7.8	60.12	10.09	25.29	1.56	49.63	36.02	122	8.68
Max	3,577	14.9	8.5	288.6	74.13	451.7	9.38	753.7	278.6	366.1	161.2
Mean	1,431	11.16	8.13	141.71	33.1	105.69	4.54	219.65	152.98	228.32	73.59
SD	620	2.04	0.19	53.99	17.51	90.47	2.1	164.53	59.17	62.13	37.67
Cv	43	18.29	2.38	38.1	52.91	85.6	46.36	74.91	38.68	27.21	51.19

Note: All values are in mg/l except pH, *T* (°C) and EC (μS/cm). WHO (2006).

Table 2
Parameter values of the three principal water groups

	Group 1					Group 2					Group 3				
	Min	Max	Mean	SD	Cv	Min	Max	Mean	SD	Cv	Min	Max	Mean	SD	Cv
EC	608	1,072	937	132	14	1,255	1,764	1,479	164	11	2016	3,577	2,403	518	22
T	8.50	14.90	11.36	2.26	19.88	7.90	13.70	11.05	1.94	17.54	8.30	13.50	10.93	1.94	17.72
pH	7.90	8.50	8.17	0.19	2.32	7.80	8.40	8.18	0.17	2.07	7.80	8.30	7.99	0.19	2.36
Ca^{2+}	60.12	270.5	119.56	48.76	40.78	76.15	236.5	138.74	42.57	30.69	130.3	288.6	193.58	50.84	26.27
Mg^{2+}	12.15	58.70	25.06	12.36	49.34	10.09	70.85	37.09	17.20	46.38	17.01	74.13	43.69	21.20	48.52
Na^{+}	25.29	99.78	53.21	18.61	34.97	59.77	232.20	106.80	56.06	52.49	105.80	451.70	215.40	128.99	59.89
K^{+}	1.56	9.38	3.98	1.98	49.65	1.56	9.38	4.30	2.25	52.22	3.91	7.82	6.11	1.46	23.93
Cl^{-}	49.63	308.4	111.75	58.62	52.46	99.27	555.9	233.51	109.95	47.08	265.9	753.70	426.41	192.42	45.13
SO_4^{2-}	36.02	240.1	134.1	51.4	38.33	52.83	273.80	140.63	57.85	41.14	163.3	278.6	213.19	37.94	17.79
HCO_3^{-}	122	366.1	244.37	67.67	27.69	122	280.7	202.3	48.64	24.04	183.1	335.6	236.48	62.61	26.48
NO_3^{-}	8.68	161.2	60.03	35.57	59.26	43.4	151.9	89.52	35.37	39.51	32.86	155	76.50	39.18	51.22

study area. The concentration in most of the northern part of the study reaches about 366.1 mg/l. The value of the chloride in the study area ranges between 49.63 and 753.7 mg/l. The value of SO_4^{2-} in the study area ranges between 36.02 and 278.6 mg/l. Almost 42% of the samples exceeded the desirable limit of Cl^-

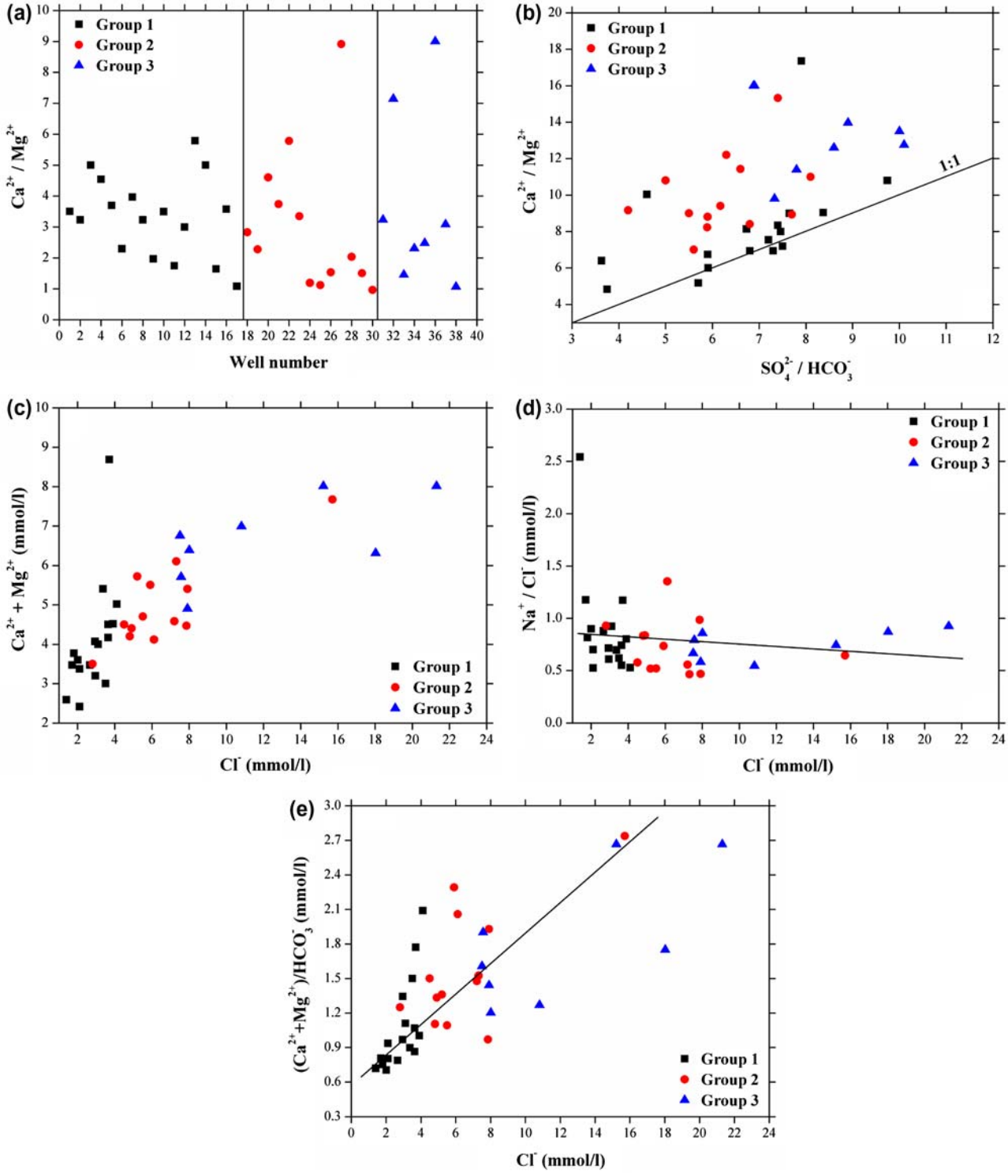

Fig. 3. Relationships of well number vs. Ca^{2+}/Mg^{2+} (a), $Ca^{2+}+Mg^{2+}$ vs. $SO_4^{2-}+HCO_3^-$ (b), $Ca^{2+}+Mg^{2+}$ vs. Cl^- (c), Na^+/Cl^- vs. Cl^- (d) and $[(Ca^{2+}+Mg^{2+})/HCO_3^-]$ vs. Cl^- (e) for waters from the study area.

(250 mg/l), but only 18.4% of them exceed that of SO_4^{2-} (250 mg/l) ([29]). Most samples exceeded the desirable limit of NO_3^- for drinking water (50 mg/l) ([29]).

4.2. Q-mode CA and water–rock interaction

In the present study, Q-mode CA was performed on the water chemistry data to group the samples in terms of water quality. The Word's method was applied and Euclidean distance was chosen as a measure of similarity. The output of the Q-mode CA is given as a dendrogram. There are three major groups shown in Fig. 2 and Table 2.

The EC of the first group of water samples (Group 1) ranges from 608 to 1,072 μS/cm, which is the characteristic of low salinity of water. Group 2 is made up of water samples of the cation composition which is dominated by Ca^{2+} and Na^{2+}, with anion composition varying from dominantly Cl^- to dominantly HCO_3^- plus SO_4^{2-}. The mean of the Group 2 is 1,479 μS/cm. The EC of the last group (Group 3) ranges from 2,016 to 3,577 μS/cm with a mean value of 2,403 μS/cm and the abundance orders are $Ca > Mg > Na > K$ and $HCO_3 > Cl > SO_4$.

The study of the Ca^{2+}/Mg^{2+} ratio of groundwater from these groups also supports the dissolution of calcite and dolomite present in the aquifer (Fig. 3(a)). That is, if the ratio $Ca^{2+}/Mg^{2+} = 1$, dissolution of dolomite should occur, whereas a higher ratio is indicative of greater calcite contribution [30]. In Fig. 3(a), the points closer to the line ($Ca^{2+}/Mg^{2+} = 1$) indicate the dissolution of dolomite. All of the samples having a ratio greater than 1 indicate the dissolution of calcite. Those with values greater than 2 indicate the effect of silicate minerals (Fig. 3(a)). Dissolved carbonates (calcite and dolomite) occur predominantly in the form of HCO_3, due to the pH range. The solubility of calcite and dolomite is largely controlled by CO_2 fugacity and pH, according to the reactions:

$$CaCO_3 + CO_{2(g)} + H_2O = Ca^{2+} + 2HCO_3^- \quad (1)$$

$$Ca_{1-x}Mg_xCO_3 + CO_{2(g)} + H_2O = (1-x)Ca^{2+} + xMg^{2+} + 2HCO_3^- \quad (2)$$

The plot of Ca^{2+}+Mg^{2+} vs. $SO_4^{2-} + HCO_3^-$ will be close to the 1:1 line if the dissolutions of calcite, dolomite, and gypsum are the dominant reactions in a system. Ion exchange tends to shift the points to the right due to an excess of $SO_4^{2-} + HCO_3^-$ [31,32]. If reverse ion exchange process take place , it will shift the points to the left due to an increase in excess of Ca^{2+}+Mg^{2+} over $SO_4^{2-} + HCO_3^-$. The plot of Ca^{2+}+Mg^{2+} vs. $SO_4^{2-} + HCO_3^-$ (Fig. 3(b)) shows that the samples of the

Table 3
Statistical summary of thermodynamic speciation calculations using PHREEQC

	Anhydrite	Aragonite	Calcite	$CO_{2(g)}$	Dolomite	Gypsum	Halite
Group 1							
Min	−2.33	0.45	0.60	−3.47	0.59	−2.08	−7.26
Max	−1.35	0.84	0.99	−2.45	1.81	−1.09	−6.47
Mean	−1.65	0.68	0.84	−2.92	1.13	−1.40	−6.88
SD	0.24	0.13	0.13	0.30	0.31	0.24	0.23
Cv	−14.72	19.29	15.80	−10.24	27.63	−17.39	−3.36
Group 2							
Min	−2.05	0.31	0.46	−3.30	−0.09	−1.80	−6.79
Max	−1.26	0.95	1.10	−2.70	1.79	−1.01	−5.50
Mean	−1.61	0.64	0.80	−3.02	1.14	−1.35	−6.26
SD	0.20	0.18	0.18	0.17	0.48	0.20	0.33
Cv	−12.59	27.65	22.33	−5.71	42.50	−14.99	−5.33
Group 3							
Min	−1.47	0.20	0.36	−2.93	0.32	−1.22	−6.11
Max	−1.23	1.08	1.24	−2.61	2.08	−0.98	−5.09
Mean	−1.34	0.62	0.77	−2.77	1.00	−1.09	−5.73
SD	0.08	0.29	0.29	0.11	0.66	0.08	0.41
Cv	−5.88	46.60	37.21	−4.08	65.43	−7.11	−7.11

second and the last groups are distributed on both sides, but reverse ion exchange process tends to dominate over ion exchange. On the other hand, most of the points of Group 1 are clustered around and above the 1:1 line. An excess of calcium and magnesium in the groundwater of Mio-Plio-Quaternary aquifer may be due to the exchange of sodium in the water by calcium and magnesium in clay material.

The plot of Ca^{2+}+Mg^{2+} vs. Cl^- (Fig. 3(c)) indicates that Ca^{2+} and Mg^{2+} increase with increasing salinity. The plots of Na^+/Cl^- vs. Cl^- (Fig. 3(d)) and Ca^{2+}+ Mg^{2+} vs. Cl^- (Fig. 3(c)) clearly indicate that salinity increases with the decrease in Na^+/Cl^- and increase in Ca^{2+}+Mg^{2+}, which may be due to reverse ion exchange in the clay/weathered layer. During this process, the aquifer matrix may adsorb dissolved sodium in exchange for bound Ca^{2+} and Mg^{2+}. The sources of Ca^{2+} and Mg^{2+} in groundwater can be deduced from the $(Ca^{2+}+Mg^{2+})/HCO_3^-$ ratio. As this ratio increases with salinity (Fig. 3(e)), Mg^{2+} and Ca^{2+} are added to solution at a greater rate than HCO_3^-.

4.3. Geochemical modeling

The saturation index (SI) of a given mineral is defined in Eq. (1) as:

$$SI = \log_{10}(IAP/K_{sp}) \quad (3)$$

where IAP is the ion activity product and K_{sp} is the solubility product at a given temperature. When the SI is below 0, the water is undersaturated with respect to the mineral in question. An SI of 0 means water is in equilibrium with the mineral, whereas an SI greater than 0 means a supersaturated solution with respect to the mineral in question. The results of saturation show that all groups are supersaturated with respect to aragonite, calcite, and dolomite (carbonate minerals) (Table 3). Anhydrite, gypsum, and halite (evaporate minerals) are undersaturated in all groups suggesting that their soluble component Na^+, Cl^-, Ca^{2+}, and SO_4^{2-} concentrations are not limited by mineral equilibrium.

Table 4
Results of inverse modeling using the means of each statistical group as input

Mineral phases	Phase mol transfers Group 1 – Group 2					
Aragonite	–	–	−1.37E−03	–	−1.37E−03	−8.44E−01
Calcite	−1.37E−03	−1.37E−03	−9.81E−04	−8.44E−01	−9.81E−04	−9.81E−04
Dolomite	3.89E−04	3.89E−04	–	2.62E−04	–	4.96E−04
Anhydrite	–	1.71E−04	–	–	1.71E−04	–
Gypsum	1.71E−04	–	1.71E−04	–	–	–
Halite	3.81E−03	3.81E−03	3.81E−03	3.41E−03	3.81E−03	3.41E−03
$CO_{2(g)}$	–	–	–	8.42E−01	–	8.42E−01
Kaolinite	−2.13E−03	−2.13E−03	−2.13E−03	−5.95E + 00	−2.13E−03	−5.95E + 00
Quartz	−2.45E−03	−2.45E−03	−2.45E−03	−6.84E + 00	−2.45E−03	−6.84E + 00
Ca-smectite	1.83E−03	1.83E−03	1.83E−03	5.11E+00	1.83E−03	5.11E+00
Ca-ion exchange	8.98E−04	8.98E−04	8.98E−04	8.41E−04	8.98E−04	8.41E−04
Na-ion exchange	−1.80E−03	−1.80E−03	−1.80E−03	−1.68E−03	−1.80E−03	−1.68E−03
Mineral phases	Phase mol transfers Group 2 – Group 3					
Aragonite	–	−2.89E−04	−2.89E−04	–	−2.89E−04	−1.33E−04
Calcite	−9.66E−05	–	−2.89E−04	–	–	−2.89E−04
Dolomite	−3.30E−04	–	–	−3.32E−04	−3.32E−04	−3.32E−04
Anhydrite	–	7.40E−04	–	–	7.85E−04	4.80E−04
Gypsum	7.88E−04			7.81E−04	5.67E−03	5.67E−03
Halite	5.71E−03	2.57E−03	5.67E−03	5.67E−03	–	4.32E−03
$CO_{2(g)}$	2.36E−05	–	2.36E−05	3.12E−04	–	3.12E−04
Kaolinite	1.97E−03	−2.17E+01	–	−2.07E+01	−2.07E+01	–
Quartz	–	−2.50E+01	–	−2.38E+01	−2.38E+01	–
Ca-smectite	–	−1.75E−03	−1.69E−03	–	−1.77E−03	–
Ca-ion exchange	6.09E−04	–	5.70E−04	–	5.70E−04	3.11E−04
Na-ion exchange	−1.22E-03	–	−1.14E−03	–	−1.14E−03	−6.23E−04

Notes: Thermodynamic database used: phreeqc.dat values are in mol/kg H_2O. Positive (mass entering water) and negative (mass leaving water) phase mole transfers indicate dissolution and precipitation, respectively. – no mass transfer.

Inverse modeling calculations were performed using PHREEQC [14]. PHREEQC was also used to calculate aqueous speciation and mineral saturation indices. Inverse modeling in PHREEQC uses the mass balance approach to calculate all the stoichiometrically available reactions that can produce the observed chemical changes between end member of waters [33]. This mass balance technique has been used to quantify reactions controlling water chemistry along flow paths [34] and quantify mixing of end member components in a flow system [35]. Minerals used in the inverse geochemical models are limited to those present in the study area [36]. The inverse model was constrained so that primary mineral phases including gypsum, anhydrite, halite, and carbon dioxide (gas) were set to dissolve until they reached saturation; and calcite, aragonite, kaolinite, quartz. and Ca-smectite were set to precipitate once they reached saturation. Cation exchange reactions of Ca^{2+} for Na^{+} on exchange sites were included in the model as a source for excess Na^{+} in groundwater.

The models in Table 3 were selected from all the possible models based on the statistical measurements calculated by PHREEQC (sum of residuals and maximum fractional error) and to represent different possible combinations of reactants and products that can account for the change in water chemistry. An inverse model describing the evolution of Group 1 to Group 2 waters (Model 1) and Group 2 to Group 3 waters (Model 2) can be written as (Table 4):

Model 1: Group 1 waters + dolomite + anhydrite + gypsum + halite + Ca-smectite + Ca from ion exchange + CO_2 gas → Group 2 waters + aragonite + calcite + kaolinite + quartz + Na loss to ion exchange

Model 2: Group 2 waters + anhydrite + gypsum + halite + Ca from ion exchange + CO_2 gas → Group 3 waters + aragonite +calcite + dolomite + kaolinite + quartz + Ca-smectite + Na loss to ion exchange

In geochemical modeling, results are dependent upon valid conceptualization of the system, validity of basic concepts and principles, accuracy of input data, and level of understanding of the geochemical processes [17]. The mass balance modeling has shown that relatively few phases are required to derive observed changes in water chemistry and to account for the hydrochemical evolution in the El Eulma plain. In a broad sense, the reactions responsible for the hydrochemical evolution in the area fall into three categories: (1) dissolution of evaporite minerals; (2) precipitation of carbonate minerals, quartz, kaolinite, and Ca-smectite; and (3) ion exchange. The mineral phases were selected based on geologic descriptions, and analysis of rocks and sediments from the area.

5. Conclusion

In this study, CA and geochemical modeling were used to evaluate variations in groundwater quality of the El Eulma area, East Algeria. Three main chemically different water types were identified by Q-mode CA based on major ion contents. Group 1 samples have a low salinity EC of 937μS/cm. When a more effective process of water–rock interaction occurs, the waters acquire greater salinity, changing in composition towards Cl^{-}–HCO_3^{-}–Ca^{2+} (Group 2) and Cl^{-}–Ca^{2+}–Na^{+} (Group 3) types. The results of saturation calculations show that all groups are supersaturated with respect to carbonate minerals. Evaporite minerals are undersaturated in all groups suggesting that their soluble component Na^{+}, Cl^{-}, Ca^{2+}, and SO_4^{2-} concentrations are not limited by mineral equilibrium. The inverse geochemical modeling demonstrated that relatively few phases are required to derive water chemistry in the area. In a broad sense, the reactions responsible for the hydrochemical evolution in the area fall into three categories: (1) dissolution of evaporite minerals; (2) precipitation of carbonate minerals, quartz, kaolinite, and Ca-smectite; and (3) ion exchange.

References

[1] E. Seyhan, A.A. van-de-Griend, G.B. Engelen, Multivariate analysis and interpretation of the hydrochemistry of dolomitic reef aquifer, Northern Italy, Water Resour. Res. 21(7) (1985) 1010–1024.

[2] M. Razack, J. Dazy, Hydrochemical characterization of groundwater mixing in sedimentary and metamorphic reservoirs with combined use of Piper's principle and factor analysis, J. Hydrol. 114(3–4) (1990) 371–393.

[3] J.L. Join, J. Coudray, K. Longworth, Using principal components analysis and Na/Cl ratios to trace ground water circulation in a volcanic island: The example of Reunion, J. Hydrol. 190(1–2) (1997) 1–18.

[4] K.M. Ochsenkuehn, J. Kontoyannakos, P.M. Ochsenkuehn, A new approach to a hydrochemical study of groundwater flow, J. Hydrol. 194(1–4) (1997) 64–75.

[5] T. Liedholz, M.T. Schafmeister, Mapping of hydrochemical ground water regimes by means of multivariatestatistical analyses, in: A. Buccianti, G. Nardi, R. Potenza (Eds.), Proc. Fourth Annu. Conf. International Association for Mathematical Geology, October 5–9, Ischia, Italy, International Association for Mathematical Geology, Kingston, pp. 298–303, 1998.

[6] Y. Wang, T. Ma, Z. Luo, Geostatistical and geochemical analysis of surface water leakage into ground water on a regional scale: A case study in the Liulin karst system, northwestern China, J. Hydrol. 246(1–4) (2001) 223–234.

[7] K.L. Locsey, M.E. Cox, Statistical and hydrochemical methods to compare basalt- and basement rock-hosted groundwaters: Atheron Tablelands, northeastern Australia, Environ. Geol. 43 (6) (2003) 698–713.

[8] S. Adams, R. Titus, K. Pietersen, G. Tredoux, C. Harris, Hydrochemical characteristics of aquifers near Sutherland in the western Karoo, South Africa, J. Hydrol. 241(1–2) (2001) 91–103.
[9] W.D. Alberto, D.M. del Pilar, A.M. Valeria, P.S. Fabiana, H.A. Cecilia, B.M. de los Angles, Pattern recognition techniques for the evaluation of spatial and temporal variations in water quality, a case study: Suquia River Basin (Cordoba-Argentina), Water Resour. 35 (2001) 2881–2894.
[10] M.A. Hernandez, N. Gonzalez, M. Levin, Multivariate analysis of a coastal phreatic aquifer using hydrochemical and isotopic indicators, Buenos Aires, Argentina, in: Proc. Int. Assoc. Water Pollution Research and Control's International Seminar on Pollution, Protection and Control of Ground Water, as published in Water Sci. Technol. 24 (1991) 139–146.
[11] M. Birke, U. Rauch, Environmental aspects of the regional geochemical survey in the southern part of East Germany, J. Geochem. Explor. 49(1–2) (1993) 35–61.
[12] B. Helena, R. Pardo, M. Vega, E. Barrado, J.M. Fernandez, L. Fernandez, Temporal evolution of ground water composition in an alluvial aquifer (Pisuerga River, Spain) by principal component analysis, Water Res. 34 (2000) 807–816.
[13] H.G. Pereira, S. Renca, J. Sataiva, A case study on geochemical anomaly identification through principal component analysis supplementary projection, Appl. Geochem. 18 (2003) 37–44.
[14] D.L. Parkhurst, C.A.J. Appelo, User's guide to PHREEQC (ver. 2)—a computer program for speciation, batch-reaction, one-dimensional transport, and inverse geochemical calculations, US Geol. Surv. Water-Res. Invest. Rept. (99-4259), 1999.
[15] S.R. Charlton, C.L. Macklin, D.D. Parkhurst, PHREEQCI—a graphical user interface for the geochemical computer program PHREEQC, US Geol. Surv. Water Res. Investi. Rept. (97-4222), 1997.
[16] C. Zhu, G. Anderson, Environmental Application of Geochemical Modeling, Cambridge University Press, Cambridge, 2002.
[17] C. Güler, G.D. Thyne, Hydrologic and geologic factors controlling surface and groundwater chemistry in Indian wells-Owens Valley area, southeastern California, USA, J. Hydrol. 285 (2004) 177–198.
[18] J. Savornin, Study of geology of the Hodna and Setif plateau, Thesis Sc. Nat. Lyon. France, 1920.
[19] J. Galcon, Research on the geology and ore deposits of the Setif Tell, Thesis Sc. Nat. Publ. Serv. Geol. From Algeria, 1967.
[20] R. Guiraud, Evolution post-triasique de l'avant pays de la chaîne Alpine de l'Algérie, d'après l'étude du bassin d'El Eulma et les régions voisines, Thèses Sc. Nat. Nice, France, 1973.
[21] J.M. Vila, Alpine chain of eastern Algeria and the Algerian-Tunisian border, Thesis Sc. Nat. Paris VI, France, 1980.
[22] APHA-AWWA-WPCF, Standard Methods for the Examination of Water and Waste Water, 19th ed., APHA-AWWA-WPCF, New York, NY, 1995.
[23] APHA, Standard Methods for Examination of Water and Wastewater, 17th ed., American Public Health Association, Washington, DC, 1989.
[24] American Public Health Association, Standard Methods for the Examination of Water and Wastewater, 19th ed., American Public Health Association, Washington, DC, 1995.
[25] L.S. Clesceri, A.E. Greenberg, A.D. Eaton, Standard Methods for the Examination of Water and Wastewater, 20th ed., American Public Health Association, American Water Works Association, Water Environment Federation, Washington, DC, 1998.
[26] D.L. Rowell, Soil Science: Methods and Applications, Longman Group Ltd., London, 1994, p. 350.
[27] J.C. Davis, Statistics and Data Analysis in Geology, Wiley, New York, NY, 1986, p. 647.
[28] STATISTICA® 5.0 for Windows, StatSoft, Inc., Tulsa OK, USDA, Natural Resources Conservation Services, 1999. Soil taxonomy: A basic system of soil classification for making and interpreting soil surveys, Agriculture Handbook No. 436, p. 871, 1998.
[29] WHO, Guidelines for Drinking-Water Quality, Recommendations, vol. 1, third ed., Word Health Organization, Geneva, 2006.
[30] A.L. Maya, M.D. Loucks, Solute and isotopic geochemistry and groundwater flow in the Central Wasatch Range, Utah, J. Hydrol. 172 (1995) 31–59.
[31] T.E. Cerling, B.L. Pederson, K.L.V. Damm, Sodium-Calcium ion exchange in the weathering of shales: Implications for global weathering budgets, Geology 17 (1989) 552–554.
[32] R.S. Fisher, W.F. Mulican, Hydrochemical evolution of sodium-sulfate and sodium-chloride groundwater beneath the Northern Chihuahuan desert, Trans-Pecos, Texas, USA, Hydrogeol. J. 10(4) (1997) 455–474.
[33] L.N. Plummer, M. Back, The mass balance approach: Application to interpreting the chemical evolution of hydrological systems, Am. J. Sci. 280 (1980) 130–142.
[34] J.M. Thomas, A.H. Welch, A.M. Preissler, Geochemical evolution of ground water in Smith Creek Valley—a hydrologically closed basin in central Nevada, USA, Appl. Geochem. 4 (1989) 493–510.
[35] C. Kuells, E.M. Adar, P. Udluft, Resolving patterns of ground water flow by inverse hydrochemical modeling in a semiarid Kalahari basin, Tracers Model Hydrogeol. 262 (2000) 447–451.
[36] L. Belkhiri, A. Boudoukha, L. Mouni, T. Baouz, Application of multivariate statistical methods and inverse geochemical modeling for characterization of groundwater—a case study: Ain Azel plain (Algeria), Geoderma 159 (2010) 390–398.